

2023 | 363

0D modeling of ignition and combustion processes for H₂/CH₄ blends in open chamber gas engines

Basic Research & Advanced Engineering - Simulation Technologies

Thomas Oppl, LEC GmbH

Michael Wohlthan, LEC GmbH

Gerhard Pirker, LEC GmbH

Andreas Wimmer, Graz University of Technology, Institute of Internal Combustion Engines and Thermodynamics

Nikolaus Spyra, INNIO Jenbacher GmbH & Co OG

This paper has been presented and published at the 30th CIMAC World Congress 2023 in Busan, Korea. The CIMAC Congress is held every three years, each time in a different member country. The Congress program centres around the presentation of Technical Papers on engine research and development, application engineering on the original equipment side and engine operation and maintenance on the end-user side. The themes of the 2023 event included Digitalization & Connectivity for different applications, System Integration & Hybridization, Electrification & Fuel Cells Development, Emission Reduction Technologies, Conventional and New Fuels, Dual Fuel Engines, Lubricants, Product Development of Gas and Diesel Engines, Components & Tribology, Turbochargers, Controls & Automation, Engine Thermodynamics, Simulation Technologies as well as Basic Research & Advanced Engineering. The copyright of this paper is with CIMAC. For further information please visit <https://www.cimac.com>.

ABSTRACT

One way to reduce greenhouse gas emissions from internal combustion engines is to use hydrogen instead of fossil fuels. Reliable combustion systems are the key to ensuring robust and stable engine operation with hydrogen. Along with experimental investigations on test beds, advanced simulation models play an important role in the development of combustion systems. The wide range of simulation tasks in engine development requires a number of different simulation methods, some of which may differ greatly in their level of detail as well as discretization depth. Calculation of a large number of variations with a feasible computational effort requires zero-dimensional simulation models.

This paper presents a predictive zero-dimensional ignition and combustion model for open chamber gas engines fueled by hydrogen that includes the most important submodels to describe the relevant processes. The model is capable of predicting pure hydrogen combustion as well as any mixture of hydrogen and methane in the range of 0-100% hydrogen share with only one set of model parameters. In the modeling process, a special emphasis is placed on the reliable prediction of ignition delay, which significantly influences the subsequent combustion. Three different approaches to modeling ignition delay are presented; the newly developed approach based on reaction kinetics appears to be the best variant.

A two-step approach to validating the model was chosen. In the first step, the ignition delay model is validated in isolation from the combustion model. In the second step, the complete physical prediction model, which consists of an ignition and a combustion model, is applied and validated against the available measurement database

1 INTRODUCTION

The decarbonization of the energy and transportation sector will be the key to keeping global warming below 1.5 degree Celsius compared to the pre-industrial average as agreed upon in the Paris agreement. In order to achieve this ambitious objective, combustion systems must be operated with low-carbon or carbon-free fuels. Therefore, pure hydrogen and hydrogen/natural gas blends to fuel the internal combustion engine (ICE) are becoming more and more attractive. Because the physical properties of hydrogen differ from those of natural gas, potential combustion concepts must be adapted.

The intensive use of simulation tools allows cost and time effective development of combustion concepts for hydrogen or hydrogen/natural gas blends. The potential and the feasibility of these concepts are assessed by using zero-dimensional (0D) simulation tools to conduct variation calculations.

Numerous approaches to 0D modeling of phenomena in the ICE exist in the literature, some of which differ significantly in their fundamentals and their applicability to a wide variety of combustion processes and fuels. Approaches for which very good results have been demonstrated sometimes show dramatic weaknesses when applied in areas for which they were not developed. The calibration of a model, whether physically based or purely empirical, is usually only valid for a limited variation range of some parameters. If a model was developed for a specific fuel and is to be used with another fuel, it is usually not sufficient to adjust only the fuel properties in the models. In most cases, complete recalibration or further development is necessary.

This paper presents a 0D simulation model of ignition and combustion in open chamber gas engines fueled by hydrogen/natural gas blends which includes the most important submodels to describe the relevant processes. In contrast to the models available in the literature, the proposed models are able to represent the combustion of pure hydrogen as well as arbitrary mixtures of hydrogen and methane in the range of 0-100% hydrogen share. In the modeling process, a special emphasis is placed on the reliable prediction of ignition delay since on the one hand it significantly influences the subsequent combustion process and on the other hand it also varies considerably due to the wide range of hydrogen share variation. The use of reaction kinetic mechanisms enables detailed modeling of ignition delay. The initial flame kernel phase and the early combustion phase are modeled based on test bench measurements from the single-cylinder engine (SCE) test bed and

measurement data. A two-stage approach is taken to validate the model. In the first stage, the ignition delay is validated in isolation from the combustion model; in the second stage, the complete physical model, which consists of an ignition delay model and a combustion model, is applied and validated against the available measurement database.

The paper is structured as follows: After an explanation of the model fundamentals and the experimental database, the focus shifts to the development of the ignition delay model. Finally, the ignition delay model and the combustion model are validated.

2 MODELING BASICS

The following section briefly explains the fundamentals underlying the ignition and combustion models. The modeling is based on a 0D model that employs a two-zone thermodynamic approach to calculate the processes in the combustion chamber. All required thermodynamic properties are determined at each time step of the analysis/simulation using the instantaneous charge composition and thermodynamic properties.

This section skips over the fundamentals of ignition delay modeling, which are the focus of this paper and thus explained in detail later in section 4.

2.1 Entrainment model

Combustion is depicted by a classical mixture-controlled entrainment model. The concept is based on a laminar folded flame front that propagates into the reaction zone following the introduction of fresh unburned charge. Due to the turbulence present in the combustion chamber, the flame front is distorted and thus enlarged, which accelerates fuel conversion. The model assumes that numerous laminar flames propagate within the reaction zone of the distorted flame front. The characteristic combustion duration is based on microturbulent eddies burning in the flame front zone at the laminar flame speed. Details on the fundamentals and equations of the entrainment model can also be found in Tabaczynski [1].

A key challenge is the appropriate modeling of the flame front propagation. The flame front surface is assumed to be hemispherical as in Auer [2], and the contact between the flame front and the wall is taken into account by a reduction factor. The reduction factor is based on the volumetric progress variable. The propagation of the flame front is scaled via the turbulent flame speed and the expansion factor according to Peters [3]. The Bargende [4] turbulence model for determining the instantaneous turbulent kinetic energy and turbulent fluctuation velocities is calibrated using

CFD results. Calculation of the input values for the entrainment model requires models for the laminar and turbulent flame speeds, where the influence of flame stretching effects for hydrogen is significant. These models are explained below.

2.2 Laminar flame speed

In the process of selecting an appropriate flame speed model, an extensive study of models available in the literature was conducted in [5]. Numerous models were assessed, their advantages and disadvantages were identified and finally it was checked how suitable they are for modeling pure hydrogen combustion and especially hydrogen-methane mixtures with a wide variation in the hydrogen share of the fuel gas (from 0 to 100%). The Witt and Griebel [6], Gülder [7], Peters [8], Verhelst [9], Bougrine [10] and Sarli and Benedetto [11] models were investigated. The correlation of Sarli and Benedetto was found to be basically suitable for reproducing the trend of reaction kinetic calculation results using the GRI3.0 mechanism correctly.

To meet the high requirements for the variability of the hydrogen share in the H₂/CH₄ mixtures as well as the wide range of parameter variations in the database, however, a new regression model was introduced in [5] that is also based on the GRI3.0 mechanism. This model was used for the calculations in this paper.

2.3 Flame stretch

The laminar flame speed is affected not only by the mixture properties but also by instabilities that occur [12]. For fuels with Lewis numbers not equal to one, as is the case for hydrogen ($Le \sim 0.3$), non-uniform diffusivities can significantly affect the stability of the flame front and thus the flame propagation speed [13,14]. The Lewis number describes the ratio of thermal diffusivity to mass diffusivity. Lewis numbers lower than one describe the destabilizing effect to the flame front. Furthermore, hydrodynamic instability (Darrieus-Landau instability) [13,14], buoyancy instability (Rayleigh-Taylor instability) and "preferential diffusion instability" [15,16] cause deviations from a planar flame front and lead to a stretched flame front. Based on the considerations of Markstein [17], the conversion of the planar flame speed s_l^0 to the stretched flame speed s_l is given by the relation

$$s_l = s_l^0 (1 - \mathcal{L}\kappa) \quad (1)$$

where κ is the stretch rate and \mathcal{L} is the Markstein length. The stretch rate can be described by the flame curvature

$$\kappa = \frac{2}{r} \frac{dr}{dt} \quad (2)$$

which gives a strong dependence of the flame radius. Thus, this effect is significant especially in the initial flame phase. The Markstein length \mathcal{L} is a function of the Lewis number, indicating a strong effect of the H₂/CH₄ blend ratio on the flame speed. The calculation of effective Lewis numbers for bi-component fuels is described in [18].

2.4 Turbulent flame speed

In internal combustion engines, the flame front interacts with the flow field and becomes more distorted as the turbulence intensity increases, leading to an increase in the size of the reaction zone. If the distorted laminar flame front propagates with the laminar flame speed, a turbulent flame speed can be determined based on continuity considerations. Several models for the calculation of the turbulent flame speed are available in the literature, e.g., the Damköhler [19], Gülder [20], Zimont [21,21] and Dinkelacker [22] models, which are all based on the turbulent fluctuation velocity and integral length and differ mainly with regard to additional terms and different parameters. Previous research [5] has shown that Zimont's model is the most appropriate for the requirements of this paper. The quantities turbulent fluctuation velocity and integral length expansion are usually calculated using a k- ϵ model [4] fitted to the results of CFD simulations. As the basis for further derivations, the 0D-TKE curve is calibrated to ensure that good agreement is achieved with the CFD results, especially at the time of inlet valve closure.

3 EXPERIMENTAL DATABASE

The measurement data used in this paper comes from a single-cylinder research engine (SCE) with a displacement of about 3 liters, a compression ratio of about 12 and a swirl concept with an Atkinson camshaft. The SCE has central mixture formation by means of a Venturi gas mixer in the intake manifold. Mixtures of natural gas and hydrogen are produced externally with a multi-component gas mixer for the experiments, which were conducted over a wide range of excess air ratios (1.3 to 3.8) at a nominal speed of 1500 rpm. Regarding the acquisition of measurement data, the cylinder pressure was recorded with a resolution of 0.1°C.A. For selected parameter variations, measurement data from ion current probes are available from earlier investigations, which were used to investigate flame propagation during the early combustion phase in more detail with eight ion current probes applied around the spark plug at a radial distance of 10 mm. A detailed description of this setup is found in [23].

In addition to excess air ratio variation, the load (IMEP) was also varied between 10 and 25 bar, the ignition timing between 5 and 20°CA before TDC (top dead center) and the hydrogen content in the mixture between 0 and 100%. In creating the variations for model development, special care was taken to vary only one parameter at a time to avoid cross-influences that could lead to misinterpretation of the flame speed model results. This strategy also makes it possible to identify critical parameter variations.

4 IGNITION DELAY

In spark ignited (SI) engines, ignition delay refers to the duration between the sparkover (ignition timing) and the first noticeable energy conversion. The spark introduces energy into the combustion chamber, leading to an increase in local temperature and thus the formation of radicals which start the chain reactions necessary for ignition. If sufficient energy is introduced into the combustion chamber, the chain branching reactions exceed the chain breaking reactions and the mixture ignites [24]. Since the flame initially propagates at the laminar flame speed and therefore comparatively slowly, there is no immediately noticeable energy conversion. Only with a larger flame radius are turbulent eddies capable of wrinkling the flame front, which causes the flame to propagate at the turbulent flame speed, which increases the energy conversion. The correct description of ignition delay is essential for 0D simulations since the ignition delay determines the position of the combustion and thus the temperature and pressure levels during the energy conversion. The great influence of the H₂ share on the ignition delay with CH₄/H₂ blends poses a particular challenge for modeling.

4.1 Analysis of experimental results

In principle, an exact experimental determination of the ignition delay ID is very challenging, but a good approximation is possible using a burn rate analysis and suitable threshold values.

The analysis is made particularly difficult by the fluctuations in the burn rate around the ignition timing (cf. Figure 1). A 1% threshold value of the maximum burn rate has proven to be a stable criterion for obtaining a value $\phi_{1\%dQmax}$ that approximates the real start of combustion ϕ_{SOC} . However, this systematically results in a slightly overestimated ignition delay $ID_{1\%dQmax}$. To obtain the real measured ignition delay ID_m , a correction by an offset ϵ is necessary:

$$ID_m = ID_{1\%dQmax} - \epsilon \quad (3)$$

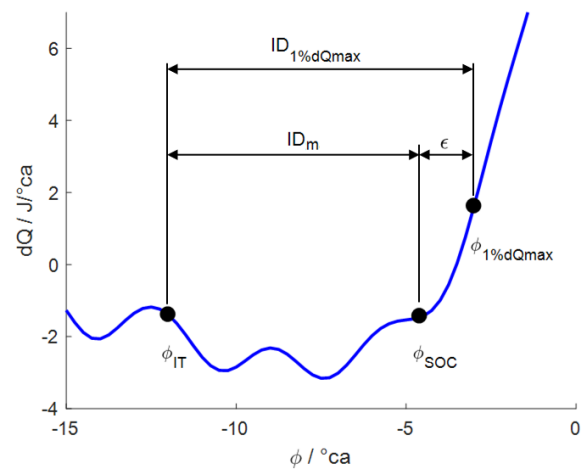


Figure 1. Determination of ignition delay based on the analyzed burn rate.

The offset can be estimated by manual analysis of a representative subdataset using visual detection of the start of combustion. As can be seen in Figure 2, the offset can be assumed to be approximately constant with $\epsilon = 2.5^\circ\text{CA}$.

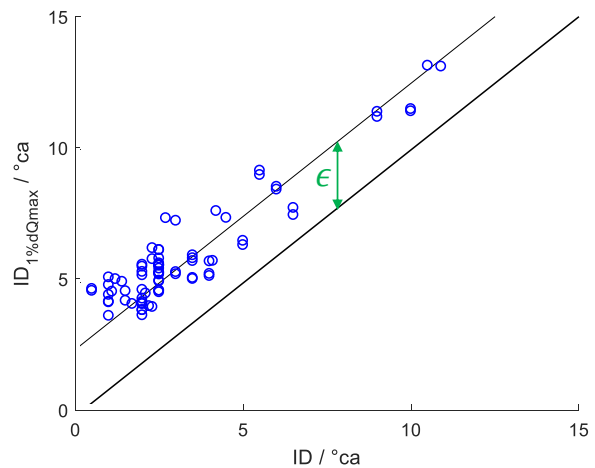


Figure 2. Determination of the ignition delay offset ϵ .

Figure 3 shows how ignition delay is greatly dependent on the excess air ratio and the hydrogen content. Pure hydrogen combustion yields the shortest ignition delay. In general, the ignition delay increases as the excess air ratio increases. This trend is particularly noticeable with hydrogen shares v_{H_2} of less than 85%, while it is weaker with higher hydrogen shares.

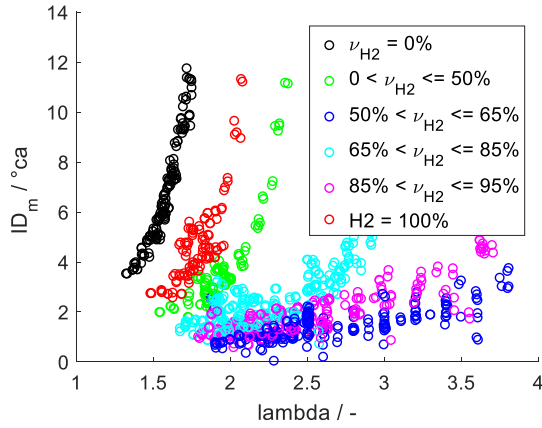


Figure 3. Measured ignition delay ID_m over excess air ratio (λ) with different hydrogen shares.

4.2 Modeling

This section outlines, compares and assesses several approaches to modeling ignition delay. Starting with a conventional approach based on the transition from laminar to turbulent flame kernel propagation, it presents a mathematical fit based on the experimental results of Figure 3 followed by a new physics-based approach that is able to describe the ignition delay with sufficient accuracy for 0-100% hydrogen share in an excess air ratio range of 1.4 to 4. The quality of the approaches is compared using root-mean-square deviation (RMSD) over n datapoints:

$$RMSD = \sqrt{\frac{1}{n} \sum_1^n (ID_m - ID_{model})^2} \quad (4)$$

4.2.1 Approach 1: Laminar/turbulent flame kernel development

While it is common practice to model ignition delay in compression ignited (CI) internal combustion engines on the basis of reaction kinetic calculations, separate modeling of ignition delay in spark ignited (SI) internal combustion engines is usually not performed. Instead, an approach is followed which describes the initial combustion phase by the transition from laminar to fully developed turbulent flame propagation [2]. This approach is based on the modeling concept that during the initial flame kernel development, the turbulent eddies are larger than the flame radius. As a result, the flame front is initially not wrinkled and the flame propagates at the laminar flame speed. As the flame radius increases, the flame front is deformed and wrinkled by the eddies. If the flame radius exceeds a critical radius, the flame propagates at the turbulent flame speed [2]. The transition from laminar flame speed s_l to turbulent flame speed s_t can be described by

$$s = s_l + \frac{(s_t - s_l)}{r_c - r_0} (r_f - r_0) \quad (5)$$

where r_f , r_c and r_0 are the flame radius, critical radius and initial flame radius. The critical radius is usually coupled with a turbulent length scale which describes the size of the eddies in the combustion chamber. Due to the slow flame propagation in the beginning, there is no noticeable increase in the burn rate during the initial combustion phase. The propagating flame causes the flame speed to increase until finally the turbulent flame speed is reached and the burn rate noticeably increases.

If ignition delay is modeled with this approach and applied to the considered database, it can be seen that the influence of the hydrogen share cannot be depicted correctly (Figure 4 and Figure 5). Figure 5 shows that the approach works best with pure methane, but large errors in the depiction of ignition delay occur with H_2/CH_4 blends.

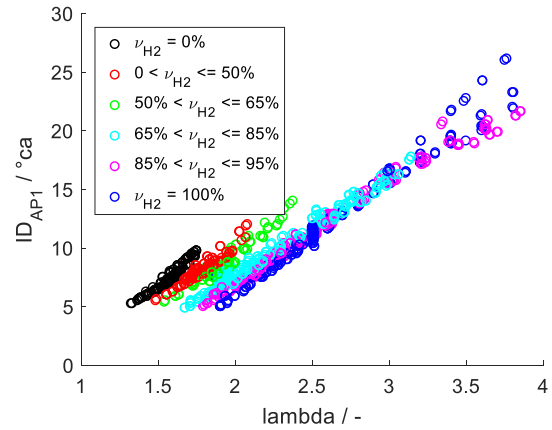


Figure 4. Results of modeled ignition delay ID_{AP1} (laminar/turbulent flame kernel development) over excess air ratio (λ) with different hydrogen shares.

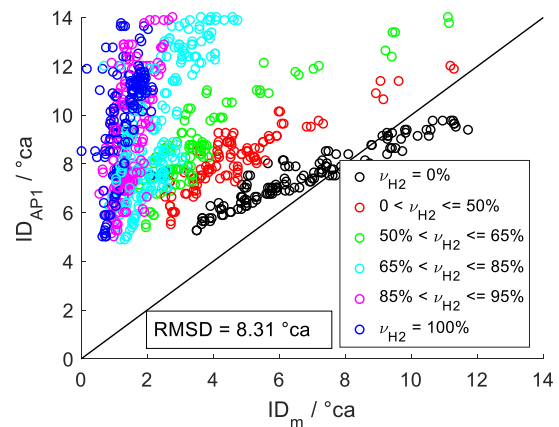


Figure 5. Results of modeled ignition delay ID_{AP1} (laminar/turbulent flame kernel development) over measured ignition delay ID_m with different hydrogen shares.

4.2.2 Approach 2: Mathematical fit

Since the approach presented above works well with pure methane but provides insufficiently precise results with H₂/CH₄ blends, this section presents a mathematical approach to modeling ignition delay. If the measured results with certain hydrogen shares are considered separately (Figure 6), the ignition delay can be described with the general approach

$$ID = a + (b + \lambda)^c \quad (6)$$

where a, b and c are model parameters and the only variable is the excess air ratio λ .

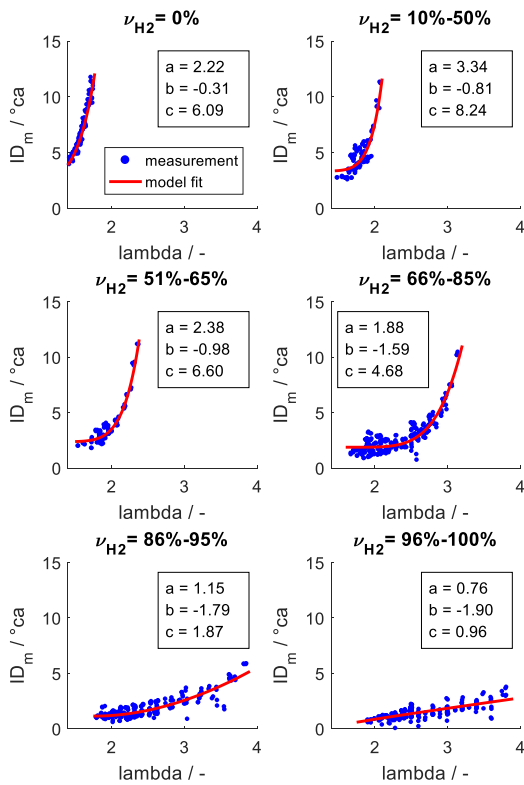


Figure 6. Model fit of different hydrogen shares over excess air ratio (lambda).

As can be seen in Figure 7, the model parameters a, b and c exhibit approximately linear behavior over the hydrogen share ν_{H_2} when the hydrogen share is greater than zero. If the parameters are each modeled with a linear dependency $p = k_p \cdot \nu_{H_2} + d_p$, the following correlation results from Eq. 6:

$$ID = k_a \nu_{H_2} + d_a + (k_b \nu_{H_2} + d_b + \lambda)^{k_c \nu_{H_2} + d_c} \quad (7)$$

Table 1 provides the calibrated parameter set for the database considered in this paper.

Table 1. Calibrated parameters for Eq. 7.

Parameter	Value
k_a	-0.038
k_b	-0.006
k_c	-0.072
d_a	3.625
d_b	-0.452
d_c	8.102

Figure 8 and Figure 9 show that with this set of parameters, the model gives a good representation of the measured ignition delay with all hydrogen shares over the entire range of excess air ratios.

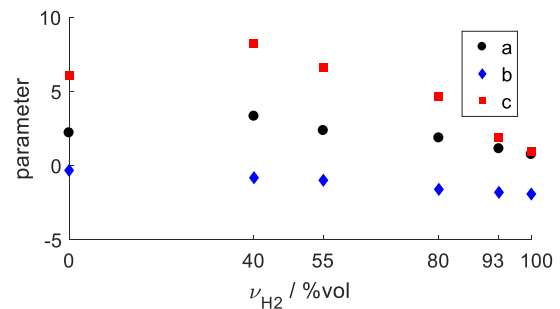


Figure 7. Model parameters of Eq. 6 over H₂ share.

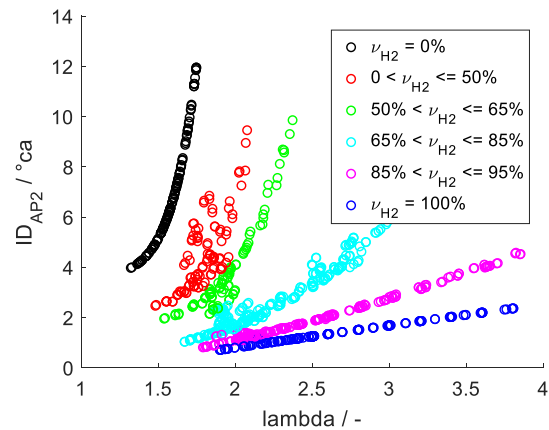


Figure 8. Results of modeled ignition delay ID_{AP2} (mathematical fit) over the excess air ratio (lambda) with different hydrogen shares.

4.2.3 Approach 3: Combination of chemical ignition delay and laminar flame kernel development

Although the mathematical fit (Eq. 7) presented above accurately models the ignition delay over the entire data range, a physical modeling approach is preferable due to its better predictive capabilities.

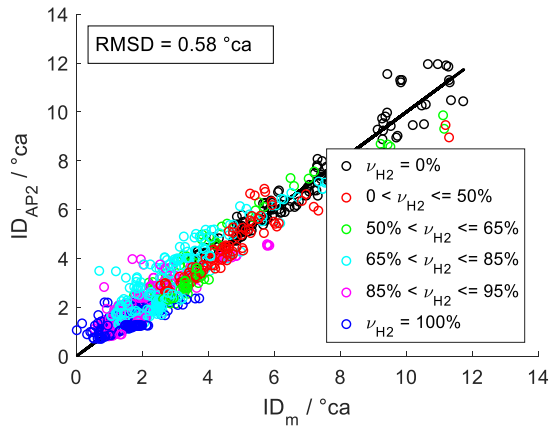


Figure 9. Results of modeled ignition delay ID_{AP2} (mathematical fit) over the measured ignition delay ID_m with different hydrogen shares.

The novel approach presented here is based on the assumption that the ignition delay is divided into two phases, a chemical phase and a laminar flame phase. In the first phase immediately after sparkover, the reaction kinetic effects dominate. Chain branching reactions in which radicals are formed take place, while the temperature of the system does not change significantly. In the second phase, laminar flame kernel development occurs, which does not lead to any noticeable energy conversion due to the low flame speed at the beginning. These two phases are combined in the ignition delay model for approach 3:

$$ID_{AP3} = ID_C + ID_L \quad (8)$$

where ID_C represents the ignition delay of the chemical phase and ID_L the ignition delay of the phase with laminar flame kernel propagation.

The chemical ignition delay is completed when the integral of the reciprocal ignition delay starting at ignition timing IT reaches the value of one:

$$\int_{IT}^{IT+ID_C} \frac{C_1}{\tau_C(t)} dt = 1 \quad (9)$$

Here, τ_C is the chemical ignition delay at a certain point in time t and C_1 is a model parameter. To calculate τ_C , reaction kinetic calculations of a zero-dimensional reactor were performed using the open-software tool CANTERA. The reaction mechanism UCS-MECH Ver. 2 [27] was used to describe the detailed reactor chemistry. Several mechanisms were investigated, including GRI-Mech3 [28], NH3-H2-CH4-Mech [29] and LNLL-Mech [30] (for H2); however, the USC-MECH was found to be the best compromise in terms of stability, computation time and accuracy. A validation of the USC-MECH showed a good agreement of the simulated and measured ignition

delays (literature values) for hydrogen shares ranging from 0% to 100%. To model the ignition spark, hot air is supplied to the reactor in the form of an air pulse at a time step $t=IT$. The air pulse has a duration of a few microseconds and is thus several orders of magnitude smaller than the chemical ignition delay. The introduced hot air initiates chemical reactions in the gas mixture and thus the ignition of the reactor charge. During chain branching reactions, the reactor temperature increases very slowly. As soon as a critical radical concentration is reached, the global reaction turnover increases explosively and leads to a strong temperature increase in the reactor. The time span between the air pulse and the maximum temperature gradient was chosen as the chemical ignition delay ID_C (Figure 10). To obtain ignition delays at different engine conditions, the initial thermodynamic state of the reactor was varied within the parameter ranges given in Table 2.

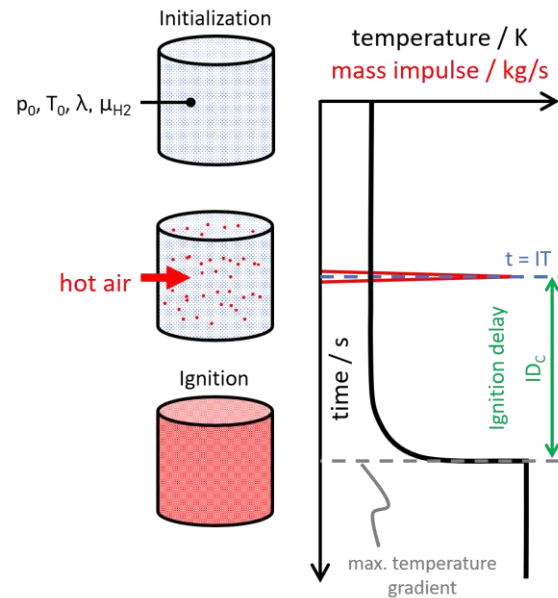


Figure 10. Principal workflow of reaction kinetic calculations and typical temperature profile for ignition delay determination.

In this model, the hot air represents the plasma core during sparkover. The state of the hot air at $t=IT$ was determined with a spark ignition model according to Meyer [31], which enables the calculation of the thermodynamic state and mass of the plasma core using pressure and temperature boundary conditions from zero-dimensional engine cycle calculation. With these results, the thermodynamic state of the reactor can be determined assuming a pressure equilibrium between the reactor and the introduced air. The only unknown that remains is the reactor volume.

Table 2. Parameter range for reaction kinetic determination of chemical ignition delays

Parameter	Unit	Range
Initial reactor temperature	K	700 ÷ 1000
Initial reactor pressure	bar	20 ÷ 100
Hydrogen share of fuel gas	%vol	0 ÷ 100
Excess air ratio	-	1 ÷ 4

To establish the reactor volume, five representative data points were selected at which the reactor volume was determined iteratively so that the calculated and measured ignition delays matched. Figure 11 shows that at these 5 data points, the determined reactor volume has an approximately constant value over a wide range of variations in ignition delay. Consequently, the further ignition delay calculations use a constant reactor volume of 1.41 mm³.

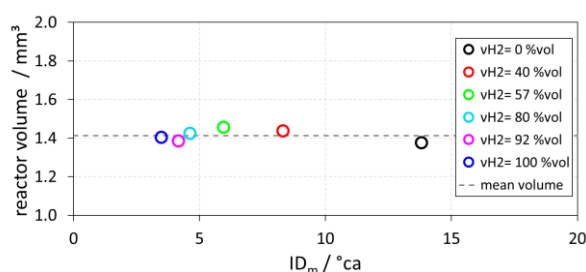


Figure 11. Reactor volume required for the model to meet the measured ignition delays ID_m.

Figure 12 shows the logarithmic results of the chemical ignition delays over pressure with different reactor temperatures and mixture compositions. For pure hydrogen (blue), the ignition delays are also shown at different excess air ratios. It can be seen that the ignition delay greatly decreases as temperature, while increasing pressure leads to longer ignition delays. In addition, hydrogen and richer mixtures accelerate the ignition process.

The phase with laminar flame kernel development begins after the chemical ignition delay at the timestep IT+ID_C and again is described by an ignition integral:

$$\int_{IT+ID_C}^{IT+ID_C+ID_L} \frac{s_l(t)}{C_2} dt = 1 \quad (10)$$

where s_l is the stretched laminar flame speed (see Eq. 1), C_2 is a model parameter and ID_L is the ignition delay of this phase. Figure 13 illustrates the importance of the flame stretching effect in proper modeling of the flame kernel propagation. While the accelerating effect of flame stretching is small with pure methane ($Le \sim 0.96$) and at low hydrogen shares, significant flame acceleration occurs with

higher hydrogen shares due to the decreasing Lewis number. With pure hydrogen ($Le \sim 0.3$), the initial flame speed almost doubles. This effect decreases as the flame radius lengthens due to the decreasing flame curvature (stretch rate, see Eq. 2), and the stretched flame speed converges with the planar one.

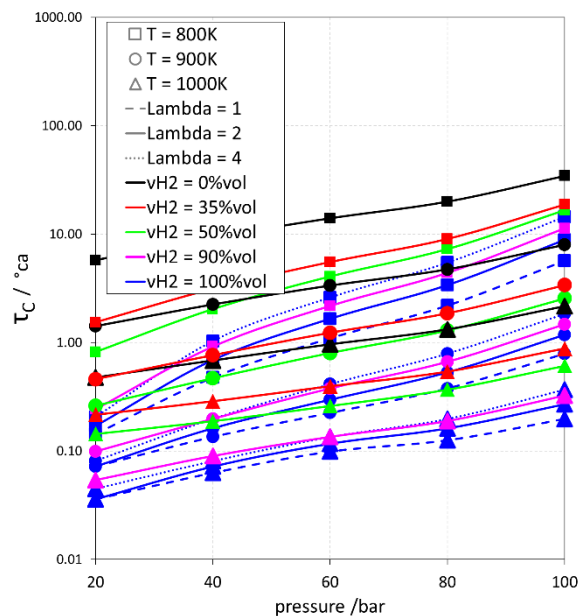


Figure 12. Chemical ignition delays τ_c under various reactor conditions.

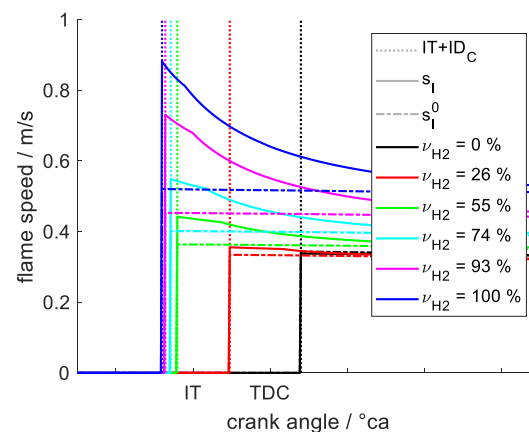


Figure 13. Comparison of planar flame speed s_l^0 and stretched laminar flame speed s_l in the initial combustion phase after chemical ignition delay IT+ID_C with different hydrogen shares.

Calibration of the model (equations 8 to 10) using the database considered in this paper yields the model parameters C_1 and C_2 . Figure 14 and Figure 15 show the results of the combined approach. The model yields good results especially in the ignition delay range from 0 to 7 °CA. At higher values, there is a tendency to underestimate the ignition delay.

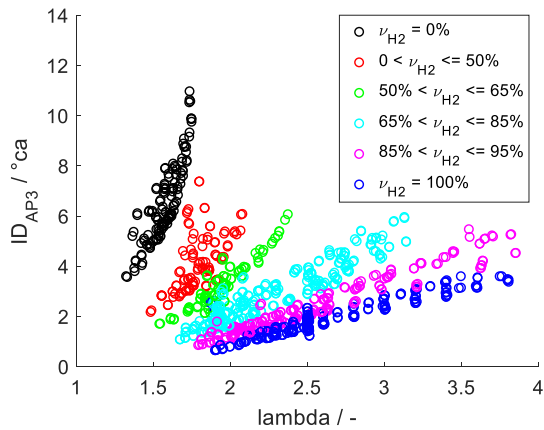


Figure 14. Results of modeled ignition delay ID_{AP3} (combined approach) over the excess air ratio (lambda) with different hydrogen shares.

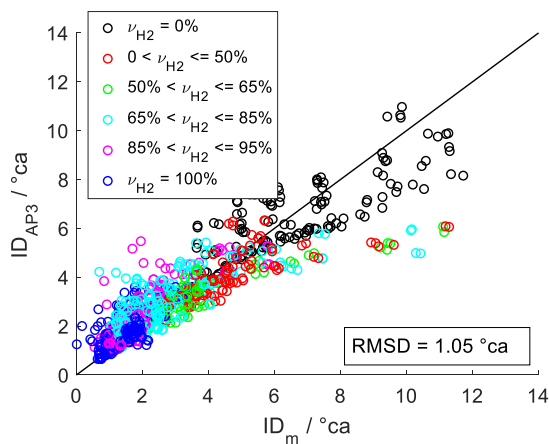


Figure 15. Results of modeled ignition delay ID_{AP3} (combined approach) over measured ignition delay ID_m with different hydrogen shares.

4.3 Comparison and discussion of the ignition delay modeling approaches

This section presents the three approaches to modeling ignition delay. While the first approach based on conventional modeling with a transition between laminar and turbulent flame core propagation does not provide sufficiently satisfactory results with the considered database, ignition delay can be satisfactorily modeled with the other two approaches. As can be seen in Figure 16, the lowest RMSD is obtained with the mathematical fit approach. However, the disadvantages of this type of modeling approach are very limited extrapolative and predictive capabilities. These drawbacks can be avoided with the newly developed physical approach (AP 3), whose RMSD is only slightly higher.

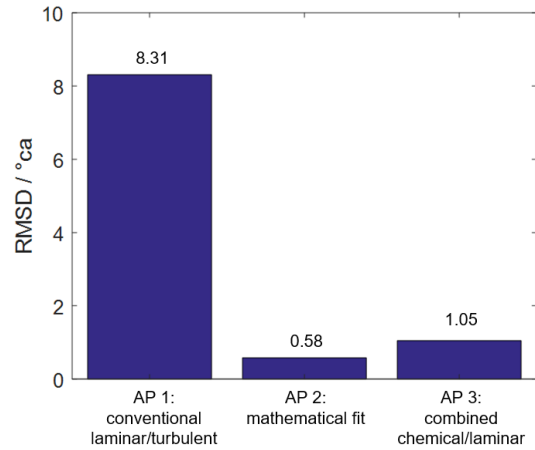


Figure 16. Comparison of the RMSD of the three modeling approaches.

5 VALIDATION OF THE BURN RATE MODEL

This section validates the overall burn rate model described in detail in [5] in combination with the novel ignition delay model (AP 3) presented above by comparing the simulated and analyzed burn rates. Figure 17 shows the model validation over a wide range of variations in hydrogen share at constant load (IMEP = 10 bar), constant ignition timing (IT = -10°CA aTDC) and constant NOx emissions (NOx = 500 mg/nm³) and Figure 18 shows the model validation for an ignition timing variation at constant hydrogen share (H₂ = 100%), at constant load (IMEP = 10 bar) and constant NOx emissions (NOx = 500 mg/nm³). In both cases, the NOx content was controlled by adjusting the excess air ratio. Finally, Figure 19 shows the model validation for a variation in excess air ratio at constant hydrogen share (H₂ = 100%), at constant load (IMEP = 10 bar) and constant ignition timing (IT = -10°CA aTDC).

Both the maximum burn rate and the ignition delay (and thus the start of combustion) can be predicted with good accuracy for most of the variations. Also, the combustion duration can be predicted with sufficient accuracy. As shown in Figure 19, the greatest deviations occur at excess air ratios above 2.8. Due to the retarded flame speed at extreme lean operation the flame/piston interaction is not depicted correctly by the model, affecting the simulated burn rate to decrease too early. Also with these points, the prediction of the burn rate is good for the early combustion phase, indicating that the used simulation model is capable to predict the combustion at various operation conditions with sufficient accuracy.

The found insufficiencies of the simulation model and the resulting deviations of analyzed and simulated burn rates may be addressed to the

flame front model used for the simulations. The flame front model is not able to depict the effects of the interaction between flame front and piston accurately for most of the variations.

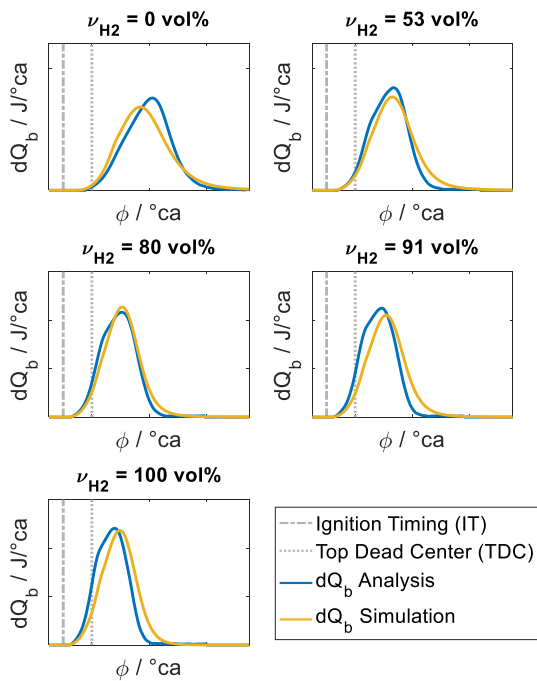


Figure 17. Comparison of simulated and analyzed burn rates when the hydrogen share is varied at IMEP = 10 bar, constant ignition timing and a NO_x level of 500 mg/nm³.

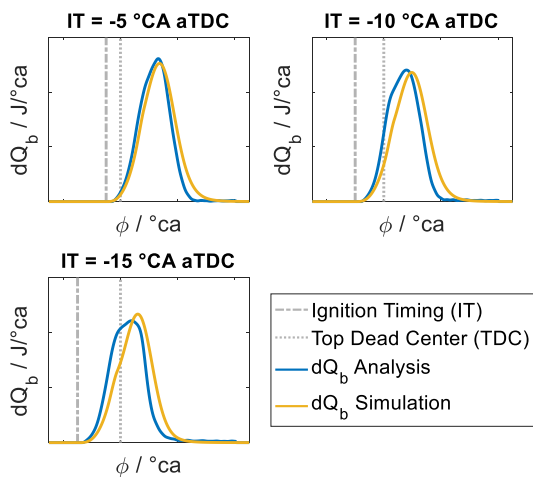


Figure 18. Comparison of simulated and analyzed burn rates when the ignition timing is varied at IMEP = 10 bar, constant hydrogen share (100%) and NO_x level of 500 mg/nm³.

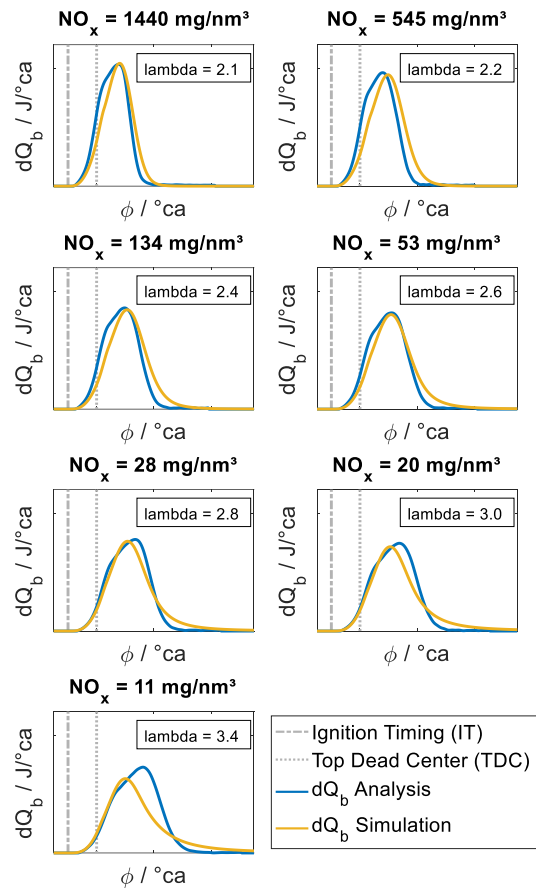


Figure 19. Comparison of simulated and analyzed burn rates when the excess air ratio (lambda) is varied at IMEP = 10 bar, constant hydrogen share (100%) and ignition timing.

6 CONCLUSIONS

In zero-dimensional simulation of the combustion of CH₄/H₂ blends, reliable modeling of ignition delay is essential for good prediction of the burn rate. This paper presented and evaluated different approaches to modeling ignition delay. It was shown that the conventional modeling approach for SI engines, which assumes a transition from laminar to turbulent flame kernel propagation, does not give sufficient results with hydrogen shares ranging from 0% to 100%.

Two newly developed approaches suitable for this application were introduced: a mathematical fit approach developed on the basis of a broad measurement database and a new physical approach based on two-phase ignition delay modeling. In the first phase, reaction kinetic processes dominate and flame kernel development does not occur yet. Afterwards, a laminar flame kernel propagates until there is a noticeable increase in the burn rate. Both approaches match the measured ignition delays well; while the

physical approach does not quite achieve the accuracy of the mathematical approach, it comes very close. Nevertheless, physics-based models are generally preferable as they have numerous advantages in terms of predictive capabilities and extrapolation capabilities. Based on the comparison between simulated and analyzed burn rates, the entire burn rate model was also sufficiently validated using the newly developed physical ignition delay model for hydrogen share variations ranging from 0% to 100% hydrogen.

7 DEFINITIONS, ACRONYMS, ABBREVIATIONS

IMEP: Indicated Mean Effective Pressure

aTDC: after Top Dead Center

bTDC: before Top Dead Center

IT: Ignition Timing

LE: Lewis number

SCE: Single Cylinder Engine

CFD: Computational Fluid Dynamics

TKE: Turbulent Kinetic Energy

SI: Spark Ignited

ID: Ignition Delay

CI: Compression Ignited

RMSD: Root Mean Square Deviation

8 ACKNOWLEDGMENTS

The authors would like to acknowledge the financial support of the "COMET - Competence Centers for Excellent Technologies" Program of the Austrian Federal Ministry for Climate Action, Environment, Energy, Mobility, Innovation and Technology (BMK) and the Austrian Federal Ministry of Labor and Economy (BMAW) and the Provinces of Salzburg, Styria and Tyrol for the COMET Centre (K1) LEC GETS. The COMET Program is managed by the Austrian Research Promotion Agency (FFG).

9 REFERENCES AND BIBLIOGRAPHY

[1] Tabaczynski, R.J., Ferguson, C.R., and Radhakrishnan, K., A Turbulent Entrainment Model for Spark-Ignition Engine Combustion, 1977, doi:<https://doi.org/10.4271/770647> UI - 770647.

[2] Auer, M., "Erstellung phänomenologischer Modelle zur Vorausberechnung des Brennverlaufes von MagerkonzeptGasmotoren", Technischen Universität München, 2010.

[3] Peters, N., "Technische Verbrennung 1, Vorlesungsskriptum".

[4] Bargende, M., "Ein Gleichungsansatz zur Berechnung der instationären Wandwärmeverluste im Hochdruckteil von Ottomotoren", Universität Stuttgart, 1990.

[5] Oppl, T., Pirker, G., Wimmer, A., Wohlthaus, M., "Zero-dimensional Modeling of Flame Propagation During Combustion of Natural Gas/Hydrogen Mixtures", SAE Technical Paper, 2023.

[6] Witt, M., Griebel, P. "Numerische Untersuchung von laminaren Methan/Luft-Vormischflammen," Villingen, Swiss, 2000.

[7] Gülder, Ö.L., Correlations of Laminar Combustion Data for Alternative S.I. Engine Fuels, 1984, doi:<https://doi.org/10.4271/841000> UI - 841000.

[8] Peters, N., "Turbulente Brenngeschwindigkeit. Abschlussbericht zum Forschungsvorhaben Pe 241/9-2," 1994.

[9] Verhelst, S., T'Joel, C., Vancoillie, J., and Demuyneck, J., "A correlation for the laminar burning velocity for use in hydrogen spark ignition engine simulation," *Int. J. Hydrogen Energy* 36(1):957–974, 2011.

[10] Bougrine, S., Richard, S., Nicolle, A., and Veynante, D., "Numerical study of laminar flame properties of diluted methane-hydrogen-air flames at high pressure and temperature using detailed chemistry," *Int. J. Hydrogen Energy* 36(18):12035–12047, 2011.

[11] Sarli, V. Di and Benedetto, A. Di, "Laminar burning velocity of hydrogen–methane/air premixed flames," *Int. J. Hydrogen Energy* 32(5):637–646, 2007, doi:<https://doi.org/10.1016/j.ijhydene.2006.05>.

[12] Verhelst, S. and Wallner, T., "Hydrogen-fueled internal combustion engines," *Prog. Energy Combust. Sci.* 35(6):490–527, 2009, doi:<https://doi.org/10.1016/j.peccs.2009.08.001>.

[13] Clavin, P., "Dynamic behavior of premixed flame fronts in laminar and turbulent flows," *Prog. Energy Combust. Sci.* 11(1):1–59, 1985.

- [14] Williams, F.A., "Combustion Theory," CRC Press, ISBN 9780429962608, 2018.
- [15] Kwon, S., Tseng, L.-K., and Faeth, G.M., "Laminar burning velocities and transition to unstable flames in H₂/O₂/N₂ and C₃H₈/O₂/N₂ mixtures," *Combust. Flame* 90(3):230–246, 1992, doi:[https://doi.org/10.1016/0010-2180\(92\)90085-4](https://doi.org/10.1016/0010-2180(92)90085-4).
- [16] Hertzberg, M., "Selective diffusional demixing: occurrence and size of cellular flames," *Prog. Energy Combust. Sci.* 15(3):203–239, 1989.
- [17] Markstein, G.H., "Experimental and Theoretical Studies of Flame-Front Stability," *J. Aeronaut. Sci.* 18:413–423, 1951.
- [18] Bouvet, N., Halter, F., Chauveau, C., Youngbin, Y., "On the effective Lewis number formulations for lean hydrogen/hydrocarbon/air mixtures", *International Journal of Hydrogen Energy*, Volume 38, Issue 14, 2013.
- [19] Damköhler, G., "Der Einfluss der Turbulenz auf die Flammgeschwindigkeit in Gasgemischen," *Zeitschrift Für Elektrochemie Und Angew. Phys. Chemie* 601–652, 1940.
- [20] Gülder, Ö.L., "Turbulent premixed flame propagation models for different combustion regimes," *Symp. Combust.* 23(1):743–750, 1991, doi:[https://doi.org/10.1016/S0082-0784\(06\)80325-5](https://doi.org/10.1016/S0082-0784(06)80325-5).
- [21] Zimont, V., Polifke, W., Bettelini, M., and Weisenstein, W., "An Efficient Computational Model for Premixed Turbulent Combustion at High Reynolds Numbers Based on a Turbulent Flame Speed Closure," *J. Eng. Gas Turbines Power* 120(3):526–532, 1998, doi:10.1115/1.2818178.
- [22] Ratzke, A., Butzbach, G., and Dinkelacker, F., "Simulating the near-wall flame extinction for gas engine application," *Proceedings of the European Combustion Meeting 2013*, 2013.
- [23] Pirker, G., Wimmer, A., Meyer, G., Kiesling, C., Nickl, A., and Tiltz, A., *Diagnostic Methods for Investigating the Ignition Process in Large Gas Engines*, 13. Int. AVL Powertrain Diagnostik Symp., 2018.
- [24] Pischinger, R., Klell, M., and Sams, T., "Thermodynamik der Verbrennungskraftmaschine, 3. Auflage," Springer, Wien, ISBN 978-3-211-99276-0, 2009.
- [25] Molina, S. & Novella, Ricardo & Gomez-Soriano, Josep & Olcina Girona, Miguel. (2021). *New Combustion Modelling Approach for Methane-Hydrogen Fueled Engines Using Machine Learning and Engine Virtualization*. *Energies*. 14. 6732. 10.3390/en14206732.
- [26] Wiese, W., Adomeit, Ph., Ewald, J. Strömungsentwicklung zur Darstellung robuster Otto-Brennverfahren. in: 11. Tagung "Der Arbeitsprozess des Verbrennungsmotors", Graz. 2007.
- [27] Wang, H., et al. "USC Mech Version II. High-temperature combustion reaction model of H₂/CO/C₁-C₄ compounds." URL: http://ignis.usc.edu/USC_Mech_II.Htm, 2007.
- [28] Smith, G.P., Golden, D.M., Frenklach, M.; Moriarty, N.W., Eiteneer, B., Goldenberg, M., Bowman, C., Hanson, R.K., Song, S., Gardiner, W.C., Lissianski, Jr. V.V. and Qin, Z., "http://www.me.berkeley.edu/gri_mech/".
- [29] Li, R., Konnov, A.A., He, G., Qin and Zhang, D., "Chemical mechanism development and reduction for combustion of NH₃/H₂/CH₄ mixtures," *Feuel*, Vol. 257, 2019, <https://doi.org/10.1016/j.fuel.2019.116059>.
- [30] O'Connaire, M., H. J. Curran, J. M. Simmie, W. J. Pitz, and C. K. Westbrook, "A Comprehensive Modeling Study of Hydrogen Oxidation," *Int. J. Chem. Kinet.*, 36:603-622, 2004 (UCRL-JC-152569).
- [31] Meyer, G., Wimmer A., "A thermodynamic model for the plasma kernel volume and temperature resulting from spark discharge at high pressures." *Journal of Thermal Analysis and Calorimetry* 133.2, 2018.

10 CONTACT

Dipl. Ing. Thomas Oppl
 Research Engineer - Simulation & Validation
 Tel.: +43 316 873-30138
 Email: thomas.oppl@lec.tugraz.at

LEC GmbH * Large Engines Competence Center
 Inffeldgasse 19, A-8010 Graz, Austria
<http://www.lec.at>